Some Peculiarities of Fatigue Crack Propagation at Different Stages of its Development

V. T. Troshchenko

G. S. Pisarenko Institute for Problems of Strength of the National Ac.Sci. of Ukraine
2 Timiryazevskaya str., Kyiv, 01014 Ukraine, e-mail address: <vtt@ipp.adam.kiev.ua>

ABSTRACT: The author considers some peculiarities of fatigue crack propagation in metals at the stages of its initiation and initial development, stable growth, and unstable growth that precedes final fracture. It is shown that at the stage of initial growth of fatigue cracks, the stress state, nonlocalized fatigue damage that precedes initiation of the main fatigue crack, residual surface stresses, surface manufacturing and in-service defects, and contact interactions are factors which determine the crack paths. Stable growth of a fatigue crack is primarily determined by the stress-strain state of a structure as a whole and by the stress-strain state at the crack tip taking into account its variation due to crack propagation, which is evaluated by the criteria of fracture mechanics. Also considered are peculiarities of fatigue crack development in compressor blades of marine gas turbines. It is shown that for embrittled steels, for which the plane strain condition is met during fatigue crack propagation, final fracture occurs at very small crack sizes. In this case, the characteristics of fatigue fracture toughness are appreciably lower than the static values. The paper also considers peculiarities of unstable fatigue crack propagation.

INTRODUCTION

The majority of failures in engineering structures are caused by fatigue of the material when fatigue crack initiation and propagation to final fracture occur in the course of cyclic loading.

In spite of a large number of researches dedicated to the investigation of fatigue crack propagation, not all aspects of this problem have been studied well enough. Specifically, the regularities of crack propagation in real structures that are the objective of this conference have not been adequately studied.

When studying the crack path, one should take into account that the mechanisms of fatigue crack propagation at various stages, namely, at the stages of crack initiation and initial growth, stable growth, and final fracture, and consequently, the regularities of their development at these stages may differ.

In this paper, with the use, in the first place, of the results of experimental studies obtained at the Institute for Problems of Strength, the author considers peculiarities of

fatigue crack path in metals under high-cycle loading at various stages of crack development considering the influence of factors important for these stages.

INITIATION AND INITIAL STAGE OF FATIGUE CRACK DEVELOPMENT

As is known, the initiation of the main fatigue crack in metal, i.e., the crack that leads to final fracture of a specimen or a component, is preceded by the stage of nonlocalized fatigue damage characterized by the presence of a large number of local zones of plastic deformation, which are centers of initiation of microscopic fatigue cracks.

As was shown in [1-3], inelastic cyclic strain per cycle at the stage of stabilization of the process of inelastic deformation is a highly efficient characteristic that allows an integral estimation of the degree of nonlocalized fatigue damage of the material, which is primarily characterized by the number and size of microscopic cracks.

Analysis made in [4, 5] revealed a clear-cut correlation between the product of the number of cracks by their average size and inelastic strain per cycle.

The size of the longest crack at stresses equal to the fatigue limit in torsion and in tension-compression, t_{-1} and s_{-1}, is taken as the size of a fatigue crack corresponding to the transition from the stage of nonlocalized damage to that of localized damage [5].

Table 1 gives us the size of such cracks for steels 45, 12KhN3A, and 40Kh tested in tension-compression and in torsion.

Table 1. Crack dimensions at stresses equal to the fatigue limit

Steel	Torsion		Tension-compression		$2l_{1tor} / 2l_{1tens}$
	t_{-1} MPa	$2l_{1tor}$ mm	s_{-1} MPa	$2l_{1tens}$ mm	
45 ($s_{0.2}$ = 339 MPa s_u = 516 MPa)	125	0.15-0.20	220	0.04-0.07	~3.20
12KhN3À ($s_{0.2}$ = 700 MPa s_u = 950 MPa)	240	0.07-0.10	395	0.02-0.036	~3.03
40Kh ($s_{0.2}$ = 683 MPa s_u = 803 MPa)	245	0.04-0.08	430	-	-

The size of such cracks decreases with increasing strength of the steels investigated. In torsion, the size of nonpropagating cracks is much larger than in tension-compression. Nonpropagating fatigue cracks are also observed at stresses below the fatigue limit, and their size decreases with increasing stresses at which they are initiated.

When testing smooth thin-wall specimens in tension-compression and in torsion, it was found [5] that a fatigue crack propagates according to the scheme shown in Fig.1.

Calculation of the stress intensity factors (SIF) K_I, K_{II}, and K_{III} for various stages of crack development was performed in accordance with the criteria of the linear elastic fracture mechanics using the results presented in [6, 7].
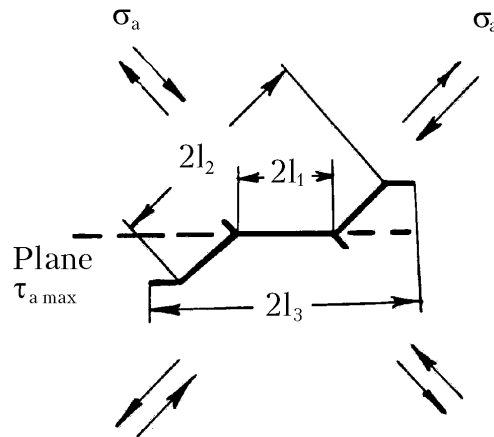

Figure 1. Scheme of fatigue crack development in torsion.

A semi-elliptical crack is initiated in the plane of maximum shear stresses. The development of the crack at the first stage ($2l_1$) is governed by the quantity K_{III}, at the second stage ($2l_2$) by K_I, and at the third stage ($2l_3$), where the crack becomes a through crack, by the quantity K_{II}. The crack dimensions and the lives corresponding to different stages of crack development in the specimens studied in torsion are listed in Table 2, where N is the number of cycles to crack initiation and N_f is the number of cycles to final fracture.

Table 2. Stages of crack propagation

Stresses	Steel 45			Steel 12KhNÇÀ			Steel 40Kh		
	Stage	$2l$ mm	N/N_f %	Stage	$2l$ mm	N/N_f %	Stage	$2l$ mm	N/N_f %
High $\left(N_f \approx 10^5\right)$	1 2 3	3.0 0 22	99.9 0 0.1	1 2 3	0.42 0.60 22	87 12.8 0.2	1 2 3	0.25 1.01 22	75 24 1
Medium $\left(N_f \approx 10^6\right)$	1 2 3	1.0 1.31 22.0	89.5 10.3 0.2	1 2 3	0.15 2.3 22	81.6 18.0 0.4	1 2 3	0.1 2.2 22	72 27 1
Below the fatigue limit at the number of cycles 5· 10^6	1 2 3	0.2 0 0	- - -	1 2 3	0.1 - -	- - -	1 2 3	0.08 - -	- - -

The results obtained in [8] revealed that an appreciable increase in the fatigue crack velocity is observed at an early stage of its development at similar values of the SIF with increasing values of cyclic stresses.

As was shown in [8], a transition of the fatigue crack propagation from the K_{III} mechanism to K_I occurs due to the fact that microcracks, oriented at an angle of 45° to the specimen axis, appear at the tip of a crack propagating by the K_{III} mechanism and will take place if, firstly, K_I is larger than the threshold stress intensity factor K_{th} ($K_I > K_{th}$), and secondly, if the rate of crack propagation by the K_I mechanism is higher than that by K_{III} mechanism. A transition of the crack propagation mechanism from K_I to K_{II} occurs in a similar way.

The governing factors in the initiation of fatigue cracks in real structures and in their development at the initial stage are the state of the surface layer and, in the first place, the presence of manufacturing and in-service defects and the magnitude, sign, and character of residual stress distribution in it.

In [9], where the authors studied fatigue crack initiation in newly-manufactured marine gas-turbine compressor blades and in those being in operation, it was shown that, owing to the influence of the aforementioned factors, fatigue cracks initiated in the blade sections wherein cyclic bending stresses were from 3 to 6.5 times lower than those in the maximally stressed root section.

In [10, 11], investigations were performed into the influence of surface defects in the form of indentor's imprints simulating dents, corrosion pits, and nonmetallic inclusions, produced on the surface by an electric-spark method, on the initiation of fatigue cracks in specimens of steels 20Kh13 and 14Kh17N2 and titanium alloy VT3-1 with different levels of manufacturing residual stresses in the surface layer in torsion and in bending.

The analysis performed revealed a very complex pattern of propagation of fatigue cracks initiated in the vicinity of defects, which depends on the type of loading, geometry of defects, the level of stress concentration, the ratio between the depth of the defect and the depth of manufacturing residual stresses in the surface layer, their sign and magnitude, etc. The manufacturing residual stresses have a particularly high impact on fatigue crack propagation in the vicinity of defects.
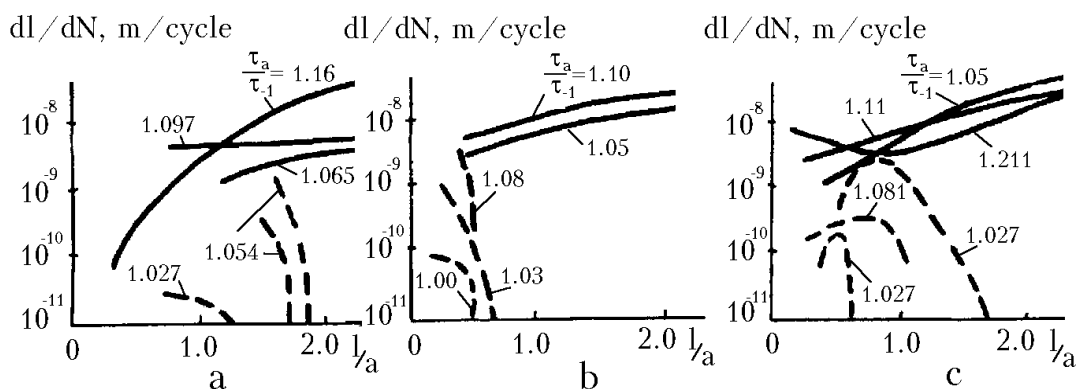

Figure 2. Kinetics of growth of fatigue cracks initiated from defects.

Figure 2 presents the kinetics of the initial growth of fatigue cracks from an indentor's imprint (a), etching pit (b), and nonmetallic inclusion (c) for specimens of titanium alloy VT3-1 under cyclic torsion in the form of relationships between the fatigue crack propagation rate dl/dN and the ratio between the crack length on the specimen surface (l) and initial size of the defect (l_0) at various relative stresses τ_a/τ_{-1}. In this figure, solid lines represent crack growth curves for defects applied to a polished surface and dashed lines for defects applied to the surface after plastic prestraining, which results in the occurrence of residual compressive stresses in the surface layer. As is seen from the figure, the presence of residual compressive stresses in the surface layer leads to retardation of crack propagation up to its complete arrest.

If residual stresses do not decelerate the crack, it propagates in the form of a semi-ellipse and acquires an energy-stable shape irrespective of the type of defect, which triggered its initiation.

A great number of papers have been dedicated to the description of the regularities in the propagation of fatigue cracks at the initial stage, which are often referred to as short cracks. Thus, in [12, 13], a relationship for the description of short fatigue cracks based on a two-parameter energy-based fracture criterion was proposed and validated by an experiment. It is shown that this relationship makes it possible to describe quantitatively the influence of the stress concentration and stress ratio in a cycle, the role of the compression part of a cycle and the state of the surface layer on crack kinetics and threshold values of the stress intensity factor, K_{th}.

The authors of [14] revealed that local cyclic plastic strains, which occur in a weakened surface layer at stresses considerably lower than the macroscopic yield strength, play an important role in the initiation and accelerated growth of short fatigue cracks. Considering this fact, they proposed a two-parameter criterion of short crack development, which incorporates the plastic strain range in the near-surface metal volume and the stress intensity factor.

Fatigue strength of materials decreases appreciably under conditions of fretting that takes place in joints, where contact surfaces slide a small distance relative to each other. Fatigue of materials under conditions of fretting has been the subject of many investigations.

The results of investigations into fatigue crack propagation in metals under conditions of fretting are presented in [15-17].

A scheme of loading and fatigue crack propagation in fretting is shown in Fig. 3, where F_σ is a variable external force, F_p is the pressure force, and $F_Q = \mu F_p$ is the friction force, where $\boldsymbol{m}$ is the coefficient of friction.

The stress intensity factors K_I and K_{II} induced by the stresses P and Q can be found with the use of the formulas given in [18].

As is shown by numerous investigations, a fatigue crack under fretting conditions is initiated on the surface and propagates according to the scheme presented in Fig. 3.

At the first stage, the crack development is defined by the shear stress intensity factor K_t whereas at the second stage, it is governed by the normal stress intensity factor K_s [18].
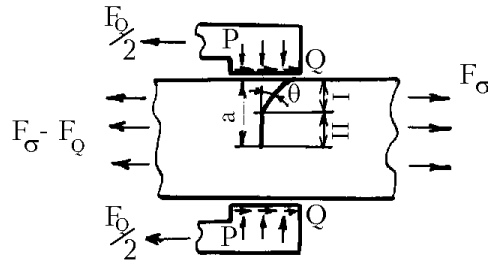
Figure 3. Scheme of loading and propagation of a crack.

In [15], a scheme of transition from the first to the second stage of fatigue crack development was proposed and justified (Fig. 4), and the conditions of fatigue crack growth arrest were formulated.
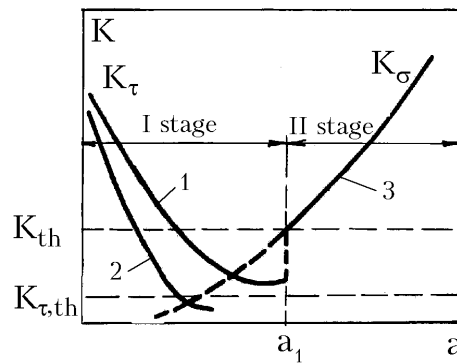

Figure 4. Scheme of transition from the first to the second stage of crack development.

In Fig. 4, curves 1 and 2 correspond to a possible variation of the K_t value as the crack extends deep into the material, curve 3 characterizes the variation of K_σ, and K_{th} and K_{th} are the threshold stress intensity factors in tension and in shear, respectively.

The conditions for transition of a crack from stage I to stage II that occurs at stresses above the fatigue limit have the following form: $K_\tau \geq K_{\tau th}$ and $K_\sigma \geq K_{th}$ (curve 1 in Fig.4).

A fatigue crack will not propagate if $K_\tau < K_{th}$ (curve 2 in Fig. 4); this condition takes place at stresses below the fatigue limit. The scheme of the fatigue crack propagation considered was validated by an experiment in [17].

On the basis of the above approach, fatigue endurance curves were plotted for a number of metals in [15, 17], and a good fit to the experimental results is shown.

A model, which allows description of the initiation and development of fatigue cracks under surface contact loading in terms of fracture mechanics, was also proposed and justified in [19]. In this model, special attention was paid to consideration of the complex stress state in the crack propagation zone that leads to a curvilinear path of

fatigue crack development. Account was also taken of stress redistribution due to the growth of cracks, their interaction, and peculiarities of changes in the loading in the contact zone.

DEVELOPMENT OF STABLE FATIGUE CRACKS

By stable fatigue cracks are meant cracks of the size when the influence of local factors such as residual surface stresses, surface manufacturing and service defects of small size, contact interaction, etc. on their development is not governing.

One of the most complicated problems in analyzing the propagation of stable cracks is to determine the SIF and other characteristics of the stress-strain state at the crack tip taking into account crack size variation in the course of its development and other factors.

Let us take as an example crack propagation in compressor blades of marine gas turbines, for which fracture by fatigue crack growth is the main one [9, 20, 21]. The design of the compressor blade investigated is given in Fig. 5 together with its cross-section. In this cross-section, we distinguish a leading (1) and trailing (2) edges, suction face (3), and pressure face (4). In operation, a compressor blade is subjected to bending vibrations (first mode, mainly). This results in the initiation of fatigue cracks in various zones of the blade section, whose development is governed by the K_I value.
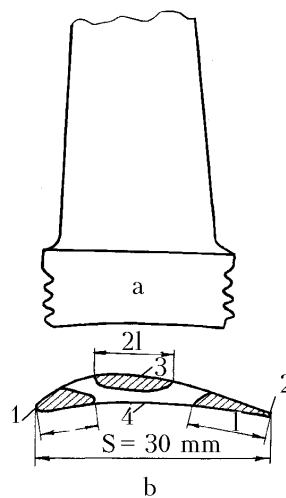

Figure 5. Scheme of a blade (a) and its cross section (b) (1 – leading edge, 2 – trailing edge, 3 – suction face, 4 –pressure face).

The blades were tested on a vibration bed under conditions of resonance at frequencies of about 700 Hz in air (*a*) and in corrosive medium (b), namely, in the vapor of the sea-salt solution corresponding to the average oceanic composition.

Investigations were performed on newly manufactured blades and on blades after being in operation for 12,000-16,000 h. The grades of steels, of which the blades were manufactured, test conditions, and the sites of fatigue crack initiation in the course of

testing are listed in Table 3. The blades whose test data are given in Table 3 differed somewhat in geometry.

For detailed studies of the regularities in fatigue crack development, surface cracks in blades on their suction surface were initiated from a drilled hole of diameter 0.2 mm and 0.3 mm in depth, cracks from the leading and trailing edges were grown from sharp notches of depth 0.2 mm. There was only one crack in each blade under study. The size of the cracks investigated varied within 0.5-15 mm.

The blade stress state was studied under static and cyclic loading taking into account the changes in the blade rigidity due to crack development.

In view of the absence of analytical methods for the determination of the SIF for cracks in blades, an experimental method was used for this purpose based on the assumption that, for the same material, equal fatigue crack growth rates correspond to equal stress intensity factors. Once crack growth diagrams for specially fabricated specimens are available, this method enables one to obtain the SIF values for any crack size in blades. A detailed justification of this method is presented in [20]. The expression for SIF calculations in corresponding blade sections has the following form:

$$K_I = Y\sigma\sqrt{2l} \, , \tag{1}$$

where σ is the bending stress in the blade, Y is a geometrical factor, and $2l$ is the crack size on the surface.

Table 3. Sites of fatigue crack initiation in blades.

Type of blade	Steel	State of blades	Test medium	Number of cracks			
				Blade suction face	Leading edge	Trailing edge	Pressure face
1	20Kh13	new	air	10	-	1	-
			sea-salt	9	2	-	1
		after opn	air	11	1	-	-
			sea-salt air	8	2	1	-
2	14Kh17N2	new	sea-salt	9	-	2	-
			air	10	3	1	1
		after opn	sea-salt	4	-	1	-
			air sea-salt	1	5	-	-
3	1Kh12N2VMF	new	air	11	-	-	-
			ñ	11	1	-	-
		after opn		10	4	1	-
				4	2	-	1

Note: new – newly manufactured blades, after opn. – blades after being in operation.

The geometrical factor in formula (1) was obtained by processing the results of calibration by the formula

$$Y = \frac{K_{\mathrm{I}}}{\sigma\sqrt{2l}} \qquad (2)$$

where K_{I} is the SIF value corresponding to a certain crack growth rate in a blade determined from diagrams plotted for the specimens tested.
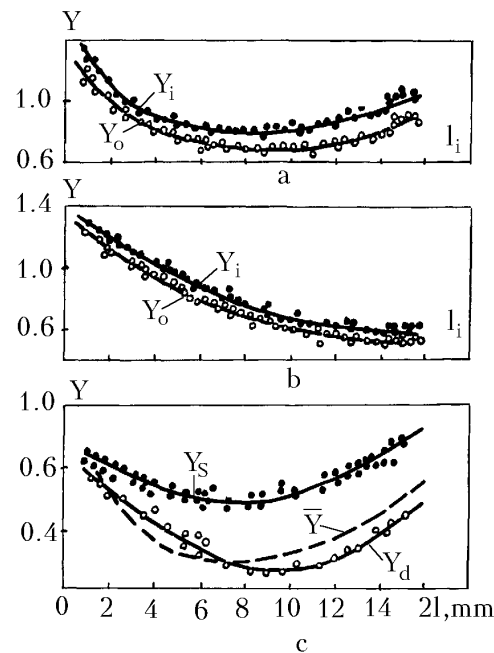

Figure 6. Experimental relations between the geometrical factor Y and the crack size.

Figure 6 presents the geometrical factor as a function of the crack size on the inner edge (l_i) when the crack propagates on the leading (Fig. 7a) and trailing (Fig. 7b) edges of a blade along their inner (Y_i) and outer (Y_o) edges and the dependences of the geometrical factor on the crack size on the suction face (Fig. 7c) when the crack propagates on the surface (Y_s) and in the bulk (Y_d) of the material [20].

The dashed line in Fig. 6c represents a similar dependence of the averaged geometrical factor $\overline{Y}$ for cracks on the suction face determined with the use of the elastic compliance method.

From Fig. 6, we can see that the magnitude of the geometrical factor, and therefore, the SIF value depend appreciably on the crack size and its location. For this reason, at the same stress state of the blade, which is characterized by the stress value in the blade, σ, and with the same crack size, the SIF value for cracks at different sites of the blade section can differ appreciably.

Figure 7 presents the results of calculations of fatigue crack nonpropagation conditions in blades of steel 14Kh17N2 for fatigue cracks propagating in the blade

section from points 1, 2, and 3. The quantity s_{th} determined by the following formula has been taken as the characteristic of crack nonpropagation:

$$\sigma_{th} = \frac{K_{th}}{Y\sqrt{2l}} \qquad (3)$$

Here, K_{th} is the threshold stress intensity factor determined when testing specimens of steel 14Kh17N2.

From the data presented in Fig.7, we can see that the lowest threshold stresses are observed when the crack propagates from the blade leading edge.
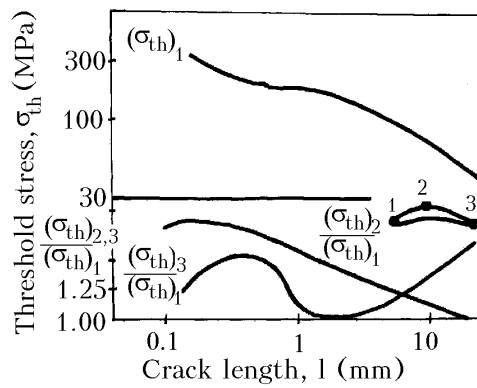

Figure 7. Conditions of fatigue crack nonpropagation in blades of steel 14Kh17N2.

The results described above reveal a complex character of fatigue crack development in structures and the dependence of their path not only on the initial stress state, which generally determines fatigue crack nucleation sites, but also on its variation in the course of crack development.

A detailed study of the kinetics of the crack shape variation was performed in [22, 23]. It was shown there that irrespective of the initial testing conditions, a fatigue crack in the course of its development tends to take a stable elliptical shape. The authors proposed a differential equation that allows prediction of the kinetics of changes in the shape of part-through fatigue cracks and showed that the best fit of the calculated and experimental results is obtained when the effective SIF values are used in that equation.

The growth of an internal flat fatigue crack in a three-dimensional body with a linear distribution of variable stresses in the crack plane and under the assumption of a penny-shaped crack and small stress gradients was considered in [24, 25]. It was shown that in the course of loading, the crack retains its shape and shifts towards the stress gradient.

The authors of [25] considered fatigue crack growth in the zone of fusion of two dissimilar materials perpendicularly to the plane of the boundary surface and showed that different characteristics of cyclic crack growth resistance of welded materials are responsible for an appreciably non-symmetrical crack growth.

In [26], it was shown that heterogeneity of the material in the weld zone could affect considerably the crack propagation kinetics in the welded joint. In particular, it was shown that in the case where the crack develops from incomplete fusion, it deviates appreciably from the initial direction towards the heat affected zone.

In [25, 27], a new integral approach to analysis of fatigue crack growth has been proposed, which is based on the use of the crack area as the main quantitative indicator of the material defectiveness and on the reduction of the equations of fatigue crack growth kinetics to relationships, which describe directly the changes in the crack area in the course of its development.

UNSTABLE FATIGUE CRACK GROWTH

Investigation of the fatigue crack propagation path is topical, first of all, where final fracture is preceded by a long stage of fatigue crack propagation and fracture occurs when fatigue crack occupies a major part of the structure cross-section. At the same time, as is shown by investigations, in some cases, fatigue fracture may take place with fatigue cracks of very small size.

Figure 8 presents temperature dependences of the ratio between the area occupied by a fatigue crack, F_c, with the number of load cycles to fracture as indicated in the figure, to the total area, F, of the cross-section of a specimen 20 mm in diameter of steel 15G2AFDps under harmonic circular bending (open symbols) and combined bending (solid symbols) when harmonic loading is superimposed by repeated impact loading [28].
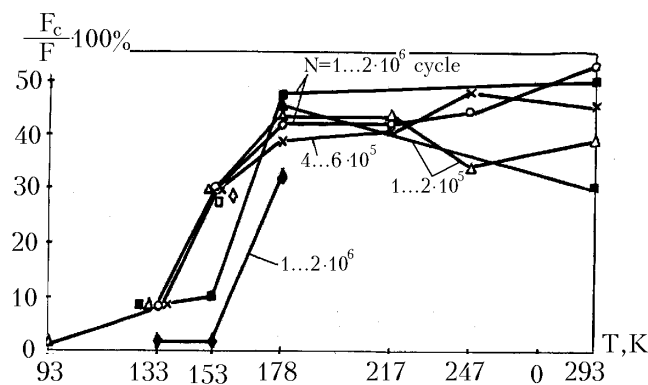

Figure 8. Relative area occupied by a crack as a function of the test temperature.

As is seen from Fig. 8, at temperatures above 180 K, a fatigue crack occupies about 50% of the specimen cross-sectional area. With a decrease in temperature down to 93 K, the area occupied by the fatigue crack decreases to 0.68% of the specimen cross-sectional area.

As was shown in [28, 29], this is attributed, first of all, to a considerable reduction in the fatigue fracture toughness, K_{fc}, with a decrease in temperature, by which we mean the maximum SIF value, which corresponds to fracture of a cracked specimen directly in the course of cyclic loading.

In [28-31], the results of fracture toughness studies under static, K_Q^{max}, and cyclic, K_{fc}, loading are reported for a heat-resistant steel in an embrittled state, heat-resistant steels at low temperatures, chrome-molybdenum steels at low temperatures, and for austenitic steels and titanium alloys, which are not embrittled with a decrease in temperature. Investigations were performed on specimens of thickness from 10 to 150 mm at various cycle stress ratios, after plastic prestraining over a wide range of primarily low temperatures.

Plane strain conditions were determined by the formula

$$t \geq 2.5 \left(\frac{K_I}{\sigma_{0.2}} \right)^2 \tag{4}$$

where t is the thickness of a compact tension specimen, K_I is the fracture toughness, and $\sigma_{0.2}$ is the offset yield stress.

The results obtained have been generalized in Fig. 9, where the ratio K_{fc}/K_Q^{max} is plotted on the vertical axis and K_Q^{max} on the horizontal axis. In this figure, points 1 correspond to heat-resistant steels, 2 to chrome-molybdenum steels, 3 to titanium alloys, 4 to austenitic steels, and 5 to carbon steel. Open symbols in this figure correspond to the results obtained when plane strain conditions were not met, solid symbols to when they were met, and half-solid symbols to when plane strain conditions were met in the determination of K_{fc} and were not met in the determination of K_Q^{max}.
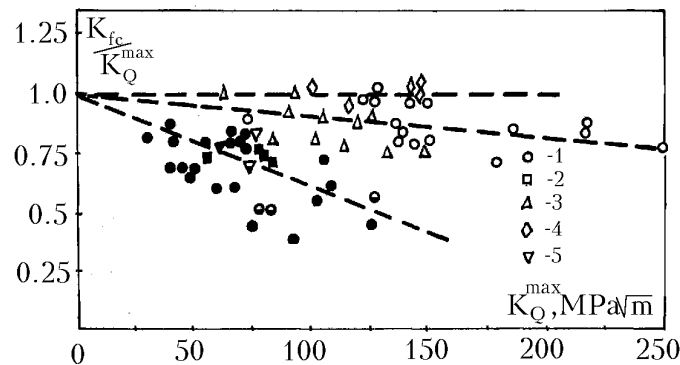

Figure 9. Comparison of static and cyclic fracture toughness characteristics.

The results given in Fig. 9 allow the following conclusions to be made.

Cyclic fracture toughness for some steels and test conditions can be much lower (by 60%) than the static fracture toughness.

The most essential reduction in the cyclic fracture toughness takes place when final fracture of a specimen under cyclic loading occurs under plane strain conditions irrespective of whether these conditions are attained by thermal treatment of the material or by lowering the test temperature.

In the case of ductile failure, cyclic fracture toughness characteristics, which in this case, can be considered only as conventional characteristics, are equal to or somewhat lower than the characteristics of the static fracture toughness.

Considering the results given in Fig. 9, the relationship between the cyclic and static fracture toughness can be presented in the form

$$K_{fc}\Big/ K_Q^{\max} = 1 - bK_Q^{\max} \tag{5}$$

where b is a parameter, which defines the intensity of the decrease in the cyclic fracture toughness with increasing $K_Q^{\max}$.

In accordance with the results presented in Fig. 9, the mean value $b \sim$ from $4 \cdot 10^{-3}$ to $5 \cdot 10^{-3}$ at fracture under plane strain conditions and $b \sim 1 \cdot 10^{-3}$ at ductile failure.

It was found [29, 30] that jumplike crack development takes place under conditions of plane strain or close to it. The values of the stress intensity factors, which trigger the onset of jumplike fatigue crack development, K_{fc}^1, are about 20% lower than those of K_{fc}. The sizes of the brittle jumps and of the zones of stable crack development in-between those jumps were found to be independent of the load cycle asymmetry and specimen dimensions and are defined unambiguously by the K_{fc}^i value, i.e., by the maximum values of the stress intensity factor in a cycle at which those jumps occur. At the same time, the number of cycles of stable crack development in-between jumps is determined by the stress intensity factor range $\Delta \mathrm{K}_{fc}^i = (1 - R)\mathrm{K}_{fc}^i$.

It was found [29] that the size of a brittle jump under plane strain conditions can be calculated by the formula

$$d_c^i = \frac{1}{3p}\left(\frac{\mathrm{K}_{fc}^i}{s_{pr}^c}\right), \tag{6}$$

where K_{fc}^i is the SIF corresponding to the crack jump, and s_{pr}^c is the cyclic proportionality limit.

The crack propagation rate during its jump was studied with the use of acoustic emission signals and was found to be as high as 150 m/s and more.

A model of transition from stable to unstable fatigue crack development was proposed and justified in [29].

REFERENCES

1. Troshchenko, V.T. (1996). In: *Multiaxial and Fatigue Design*, pp.335-348, Pineau, A., Cailletaud, G. and Lindley, T.C. (Eds), Mechanical Engineering Publication, London.
2. Feltner, G.E. and Morrow, J.D. (1961). *Trans. ASME (D)*, **81,** No**.** 1, 15-22.
3. Klesnil, M. and Lukas, P. (1980). *Fatigue of Metallic Materials*, Academia, Prague.
4. Troshchenko, V.T. (1981). *Deformation and Fracture of Metals under High-Cycle Loading* (in Russian)*,* Naukova Dumka, Kiev.
5. Troshchenko, V.T. and Dragan, V.I. (1982*). Probl. Prochn*., No. 5**,** 3-10.
6. Emery, S. (1972). *Trans. ASME (Ser.D),* No. 2, 143-151.
7. Lakshminarayana, H.V. and Murthy, M.V. (1976). *Int.J.Fract.,* **12**, No. 4, 547-566.
8. Dragan, V.I. and Yasniy, P.V. (1983). *Probl. Prochn.,* No. 8, 10-15.
9. Troshchenko, V.T., Prokopenko, A.V., Torgov, V.N., et al. (1981). *Probl. Prochn.*, No. 4, 5-10.
10. Troshchenko, V.T., Prokopenko, A.V. and Lyalikov, S.M. (1989). *Probl. Prochn.,* No. 8**,** 10-15.
11. Troshchenko, V.T. and Lyalikov, S.M. (1996). *Probl. Prochn.,* No. 1**,** 5-16.
12. Vasyutin, A.N. (1990). *Probl. Prochn.,* No. 9**,** 3-8.
13. Vasyutin, A.N. (1990). *Probl. Prochn.,* No. 9**,** 8-11.
14. Prokopenko, A.V. and Chernysh, O.N. (1989). *Probl. Prochn.,* No. **5,** 12-16.
15. Troshchenko, V.T., Tsybanev, G.V. and Khotsyanovsky, A.O. (1988). *Probl. Prochn.,* No. 6**,** 3-8.
16. Troshchenko, V.T. (2000). In: *Proc. III Intern. Symp. on Tribo-Fatigue* (ISTF-2000), pp.44-50, Oct. 22-26, 2000. Beijing, China.
17. Troshchenko, V.T., Tsybanev, G.V. and Khotsyanovsky, A.O. (1994). *Fatigue Fract. Engng. Mater. Struct.*, **17**, No. 1, 15-23.
18. Rooke, D. and Jones, D.A. (1997*). Farnborough Techn. Rep.* RAE 77181. 25.
19. Panasyuk, V.V., Datsyshyn, O.P. and Marchenko, H.P. (1995). *Eng. Fract. Mech.*, **52**, No. 1, 179-191.
20. Prokopenko, A.V. (1981). *Probl. Prochn.*, No. 4, 105-111.
21. Troshchenko, V.T. and Prokopenko, A.V. (2000). *Engng Failure Analysis*, **7**, 209-220.
22. Varfolomeev, I.V., Vainshtok, V.A. and Krasowsky, A.Ya. (1990). *Probl. Prochn.*, No. 8**,** 3-10**.**
23. Varfolomeev, I.V., Vainshtok, V.A. and Krasowsky, A.Ya. (1990). *Probl. Prochn.*, No. 9, 11-16.
24. Andreykiv, A.E., Darchuk, A.I. and Sytosenko, V.V. (1987). *Phyz.-chim. Mekh. Materialov*, No. 6, 80-83.

25. Panasyuk, V.V., Andreykiv, O.Ye., Darchuk, O.I. and Kuzniak, N.V. (1994). In: *Handbook of Fatigue Crack Propagation in Metallic Structures*, pp.1205-1242, Carpinteri, A. (Ed.), Elsevier Science B.V., Amsterdam.

26. Panasyuk, V.V., Andreykiv, O.Ye. and Lishchynska, M.V. (2000). In: *Proc.14th European Conf. on Fracture* (ECF-14), vol.II, pp. 601-608, Engng Materials Advisory Services, Ltd, Warley.

27. Andreykiv, O.Ye. and Darchuk, O.I. (1993). *Phyz.-khim. Mekh. Materialiv*, No. 4, 7-12.

28. Troshchenko, V.T. and Pokrovsky, V.V. (1975). *Probl. Prochn.*, No. 10, 8 –11.

29. Troshchenko, V.T., Pokrovsky, V.V. and Prokopenko, A.V. (1987). *Crack Resistance of Metals under Cyclic Loading*, Naukova Dumka, Kiev.

30. Troshchenko, V.T., Pokrovsky, V.V. and Yasniy, P.V. (1994). *Fatigue Fract. Engng. Mater. Struct.*, **17**, No. 9, 991-1001.

31. Troshchenko, V.T. and Pokrovsky, V.V. (1999). *Engineering Against Fatigue*, p.269-276. A.A. Balkema.